J.W. PAPPIN B.E., M.E., Ph.D., C.Eng., M.I.C.E.
B. SIMPSON M.A. Cantab., Ph.D., C.Eng., M.I.C.E.
P.J. FELTON B.Sc., M.Sc., A.M.I.C.E.
C. RAISON B.Eng., M.Sc., C.Eng., M.I.C.E.

Ove Arup & Partners, London

NUMERICAL ANALYSIS OF FLEXIBLE RETAINING WALLS

SYNOPSIS

A numerical method for analysing the behaviour of flexible retaining walls which allows soil-structure interaction to be modelled is presented. The method differs significantly from the traditional subgrade reaction approach in the ways that the soil stiffness and earth pressure limits are modelled. Three stiffness matrices are used in the analysis. One matrix represents the wall in bending while the other two represent the soil on each side of the wall. Each soil stiffness matrix is assembled using pre-calculated flexibility matrices obtained from finite element computations for elastic soil blocks. Earth pressure limits are determined from consideration of forces applied to the soil which allows the known effect of soil arching to be modelled. This occasionally permits pressures to locally exceed active and passive limits. The analysis has been incorporated into a computer program which is sufficiently economic and simple to be used as part of the general design process. Examples of its use are given.

1 INTRODUCTION

Retaining walls are often used to form the perimeter support to cutting or basement excavations. However the approach adopted for the analysis and design depends on whether the wall behaviour is essentially rigid, as for gravity retaining structures, or relatively flexible, such as sheet piles, diaphragm or secant pile walls.

Gravity walls provide restraint to the retained soil by mobilising gravity and friction forces at the base of the wall. However these walls are

often unable to develop high bending or shear stress because of excessive displacement of the foundation soil, sliding or rotation resulting in fully active conditions behind the wall. Analysis of the stability of these walls is usually carried out by the traditional Rankine or Coulomb approach and little attention is paid to prediction of movement.

Flexible retaining walls however support the ground adjacent to the excavation by transmitting predominantly horizontal earth pressures either into struts or anchors or into the soil at greater depth and are often subject to high bending and shear stresses. These stresses result in a relatively flexible behaviour and a complex soil-structure interaction. Traditionally, analysis and design of flexible retaining walls has been carried out assuming limit pressures, active behind the wall and passive in front, to determine the required penetration of the wall, and applying empirical rules to determine movements, bending moments and shear forces. While this is usually adequate to determine the necessary penetration, the empirical methods are often not sufficiently accurate and in some cases are not applicable. The wall movements, bending moments and shear forces are very dependent on the stiffnesses of the wall, struts and the soil. In addition, the stress changes applied to the soil frequently give rise to plastic failure within parts of the soil.

To investigate the behaviour of flexible retaining walls at working stresses and to predict wall and ground movements has generally involved the use of non linear finite element methods. However for routine analysis within the design office finite element methods tend to be expensive and complex and therefore susceptible to error. Consequently a simpler analysis system is desirable.

This paper describes an alternative method of analysis that has been incorporated into a computer program that is sufficiently simple and inexpensive that it can form part of the general design process. Although there are many computer programs available which can be used to investigate the behaviour of flexible walls the method of analysis presented here differs significantly from these in the way the soil stiffness and earth pressure limits are modelled. Soil stiffnesses

are modelled using pre-calculated flexibility matrices obtained from finite element computations for elastic soil blocks. The earth pressure limits allow for the known effect of soil arching in addition to the active and passive pressure limits. The analysis is sufficiently versatile to deal with most commonly encountered situations, where flexible retaining walls may be used. It is able to deal with the following:

a) soil layering including different materials on opposite sides of the wall
b) changes in soil properties at any stage
c) geometrical limits to the problem including a rigid base or vertical boundary such as the centre line of a trench
d) pore water pressure which can be either hydrostatic or directly specified
e) surcharges, either uniformly distributed loads or strip loads which can be added or removed at any stage
f) excavation or filling, soil can be added or removed from either side of the wall
g) anchors or struts can be installed or removed at any stage
h) wall stiffness can be changed at any stage

The paper also presents examples of the use of the analysis in the general design process which illustrates the range of situations that can be dealt with.

2 DESCRIPTION OF THE ANALYSIS

The analysis described below is carried out in a similar manner to more rigorous finite element computations used to investigate the behaviour of flexible retaining walls. Both analyses are carried out in steps corresponding to the proposed stages of excavation and construction. As an example, typical stages of construction that the analysis can model are shown in Figure 1. At each stage the incremental displacements due to the changes caused by that stage are calculated and added to the existing displacements. The soil stresses, strut forces, wall bending moments and shear forces can then be determined.

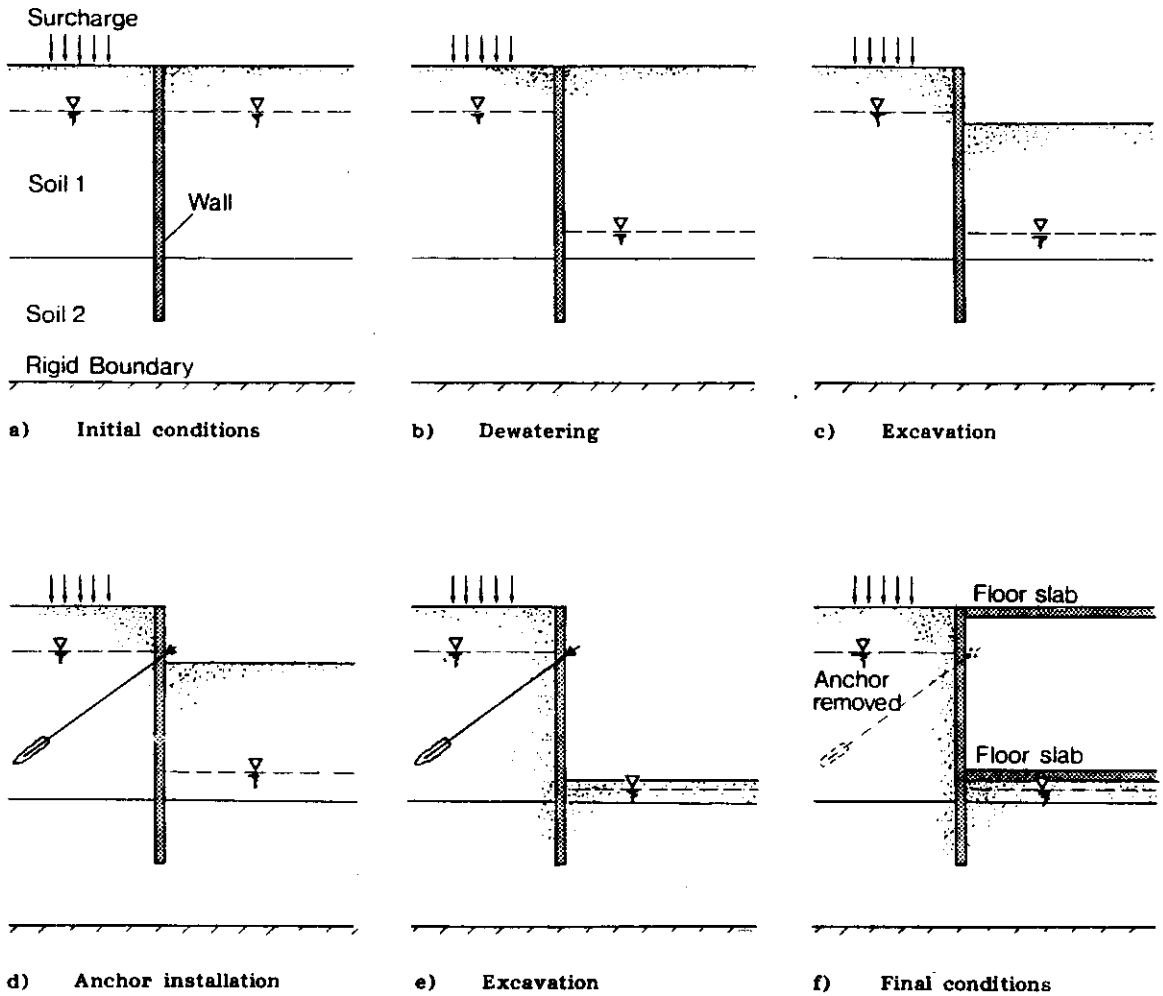

Figure 1 Typical stages of construction

2.1 Numerical Representation

The numerical representation is shown on Figure 2. The wall is modelled as a series of elastic beam elements joined at the nodes. The lowest node is either the base of the wall or at a prescribed rigid base in the ground beneath the wall. The soil to each side of the wall is connected at the nodes as shown on the figure. Only horizontal forces can be transmitted between the soil and the nodes and these forces are directly related to the earth pressures. Struts or anchors are modelled as forces and spring stiffnesses connected to the appropriate nodes.

The analysis assumes plane strain conditions but axisymmetric conditions can be approximated by suitable choice of dimensions for the soil blocks.

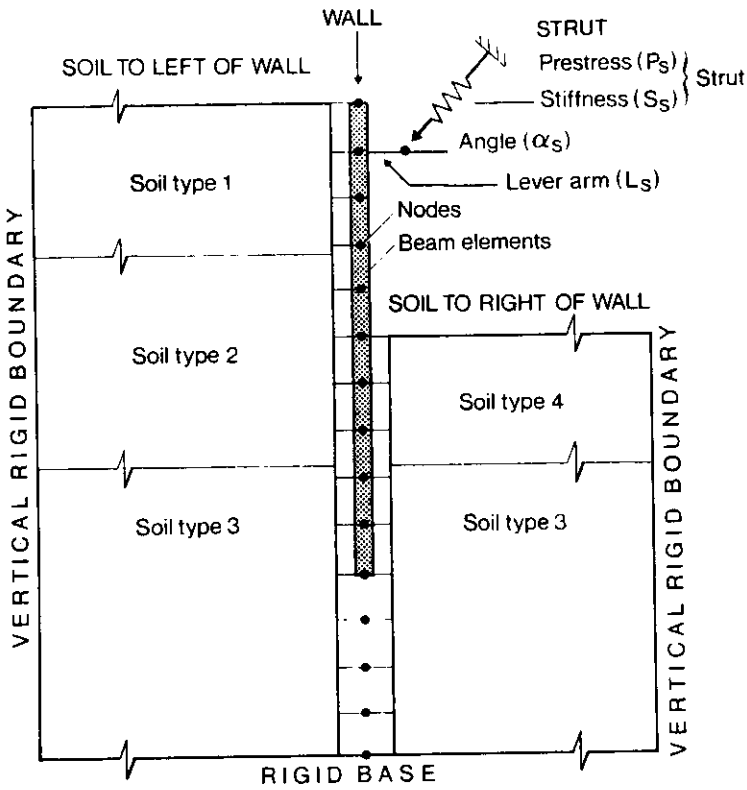

Figure 2 Numerical representation

2.2 Method of Analysis

At each stage of construction the analysis comprises the following steps:

(a) The initial earth pressures and the out of balance nodal forces are calculated assuming no movement of the nodes.

(b) Stiffness matrices representing the soil on either side of the wall and the wall itself are assembled.

(c) These matrices are combined, together with any stiffnesses representing the actions of struts or anchors, to form an overall stiffness matrix.

(d) The incremental nodal displacements are calculated from the nodal forces acting on the overall stiffness matrix assuming linear elastic behaviour.

(e) The earth pressures at each node are calculated by adding the changes in earth pressure due to the current stage to the initial earth pressures. The derivation of the changes in earth pressure includes multiplying the incremental nodal displacements by the soil stiffness matrices.

(f) The earth pressures are compared with soil strength limitation criteria conventionally taken as either the active or passive limits. If any strength criterion is infringed a set of nodal correction forces is calculated. These forces are used to restore earth pressures which are consistent with the strength criteria and also model the consequent plastic deformation within the soil.

(g) A new set of nodal forces is calculated by adding the nodal correction forces to those calculated in step (a).

(h) Steps (d) to (g) are repeated until convergence is achieved.

(i) Total nodal displacements, earth pressures, strut forces and wall shear stresses and bending moments are calculated.

Details of the above steps are given in the following sections.

2.3 Wall Stiffness

The wall is modelled as a series of elastic beam elements, the stiffness matrix being derived using conventional methods from slope deflection equations.

The moments [M] and horizontal forces [P] at the nodes are represented as

$$[M] = [A][\delta] + [B][\theta] \quad (1)$$

and $$[P] = [C][\delta] + [A]^T[\theta] \quad (2)$$

where [A], [B] and [C] are functions of the element lengths and flexural rigidity (EI), and $[\delta]$ and $[\theta]$ are the nodal horizontal displacements and rotations.

As there are no moments applied to the wall $[\theta]$ can be eliminated to give

$$[P] = [S]\ [\delta] \quad (3)$$

in which [S] is the wall stiffness matrix given by

$$[S] = [C] - [A]^T[B]^{-1}[A] \quad (4)$$

2.4 Soil Stiffness

Formulation of stiffness matrices to represent the soil on either side of the wall is not as straightforward as for the wall. As a first approximation the behaviour of the soil can be represented by linear elastic springs connected to the wall at node points. This subgrade reaction method is used in many existing computer programs. However, the method is unrealistic because it is unable to model the fact that movement at one level of the wall will cause change of earth pressures at other levels. In addition there is no satisfactory theory by which the modulus of subgrade reaction can be derived for the soil.

In order to overcome the disadvantages of using a subgrade reaction method the soil can be modelled as an elastic continuum whose stiffness can be determined by Young's modulus which may vary with depth. The present computer program, in addition to a subgrade reaction model, provides two alternative methods to the designer for deriving a stiffness matrix from the assumed soil stiffness. Both methods represent the soil either side of the wall as elastic blocks the dimensions of which can be defined by the user.

The first method, which can only be used for soil with Young's modulus constant with depth, uses the integrals of the Mindlin equations which were published by Vaziri et al (1982). This method was developed in an attempt to be able to model three dimensional situations where the assumptions of plane strain conditions do not hold. This method is discussed in more detail by Pappin et al (1985).

The second method provided by the program obtains stiffness matrices by inverting flexibility matrices derived from a combination of pre-calculated flexibility matrices. These have been calculated using plane strain finite element computations for two different elastic blocks (see Figure 3), one with uniform Young's modulus with depth and the

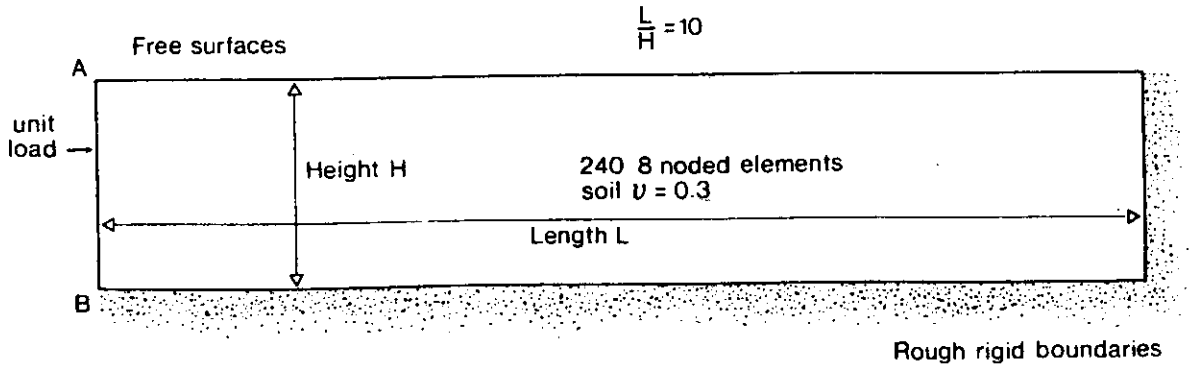

Figure 3 Elastic soil block used for finite element computations

other with Young's modulus increasing linearly with depth from zero at the surface. These flexibility matrices define the magnitude of the horizontal displacements at all the nodes on the vertical free surface due to a unit load applied at any one node. The flexibility matrices from the two cases are combined proportionally to cover any situation in which stiffness increases linearly with depth, whatever the value at the free surface. No theoretical basis has been found to confirm that such a combination would give an accurate result, but comparison with more rigorous finite element studies suggests that the approximation is, in fact, very good.

The finite element flexibility matrix is then used to generate an equivalent flexibility matrix compatible with the node spacing used to represent the wall. This manipulation is achieved by scaling the finite element mesh to match the height of the elastic soil block and then linearly combining the flexibility terms to produce the desired matrix. Special attention has been paid to achieving good approximations for the dominant terms on the leading diagonal of the matrix.

Linear variation of stiffness with depth can often oversimplify the design profile and therefore an approximate method of adjusting the matrices to accommodate non-linear variations of soil stiffness was developed. This method calculates a best fit linear Young's modulus profile E_z^* to represent the actual variation E_z (Figure 4a). The flexibility matrix [F*] corresponding to the linear approximation can then be derived from the pre-calculated matrices as described above.

In order to adjust this matrix to obtain the flexibility matrix [F] corresponding to the actual variation of Young's modulus each term in row i of [F*] is multiplied by a coefficient A_i. To maintain symmetry, terms F^*_{ij} and F^*_{ji} are both multiplied by the same coefficient, chosen as the smaller of A_i or A_j.

A number of alternative means of deriving coefficient A_i have been attempted based on consideration of the different distribution of work done due to unit load acting on two elastic soil blocks with Young's modulus profiles E^*_z and E_z. The following expression has been developed for the coefficient A_i acting at node i

$$A_i = \frac{\displaystyle\int_{Z=0}^{H} \frac{E^{*2}_z}{E_z}\left[\frac{\partial \delta^*_{zi}}{\partial z}\right] dz}{\displaystyle\int_{Z=0}^{H} E^*_z\left[\frac{\partial \delta^*_{zi}}{\partial z}\right] dz} \qquad (5)$$

where δ^*_{zi} is the displacement at depth z of the elastic soil block with Young's modulus profile E^*_z due to unit load at node i. No rigorous theoretical justification for this expression is available. However comparison between finite element solutions and those produced by this approximation have been carried out and have shown that for most practical situations errors will rarely exceed 20%. As an example, Figure 4 shows one of the more severe cases that could be envisaged. The displacement of the elastic soil block with Young's modulus profile E_z due to unit load at three different levels is shown compared against rigorous finite element solutions.

It should be noted that the pre-calculated flexibility matrices were derived for only one specific geometry which represented a length to height (L/H) ratio of 10 (see Figure 3). However most practical situations will result in different L/H ratios. This change in geometry

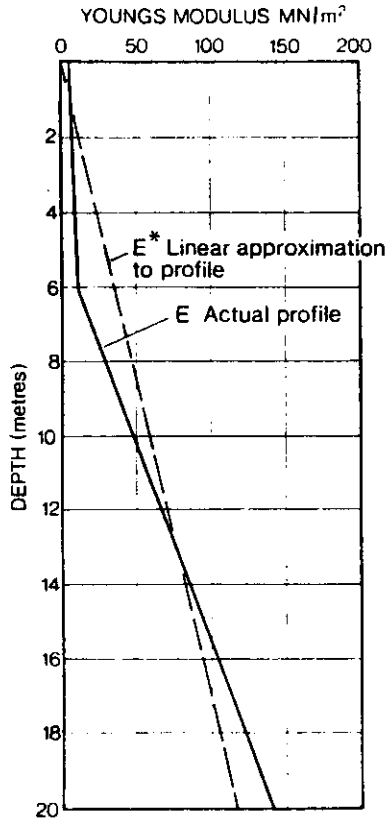

a) Soil stiffness profile

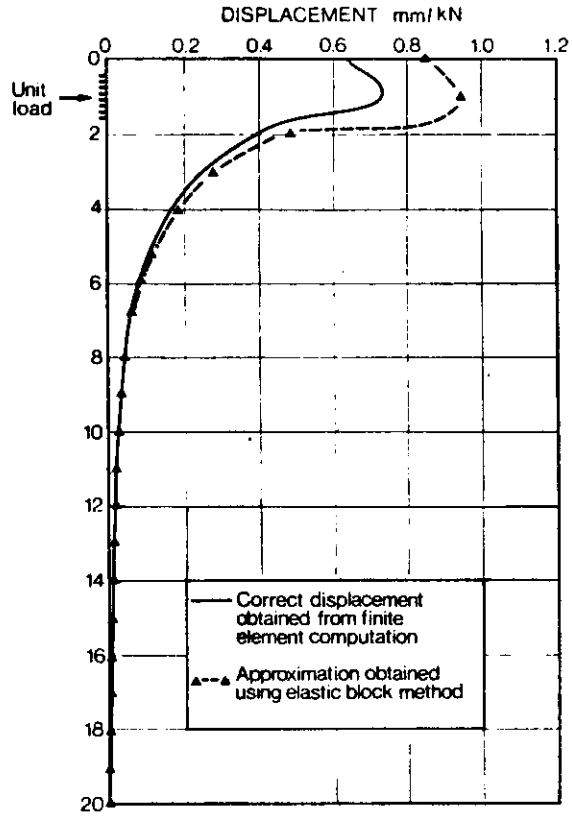

b) Displacement due to unit load at 1m depth

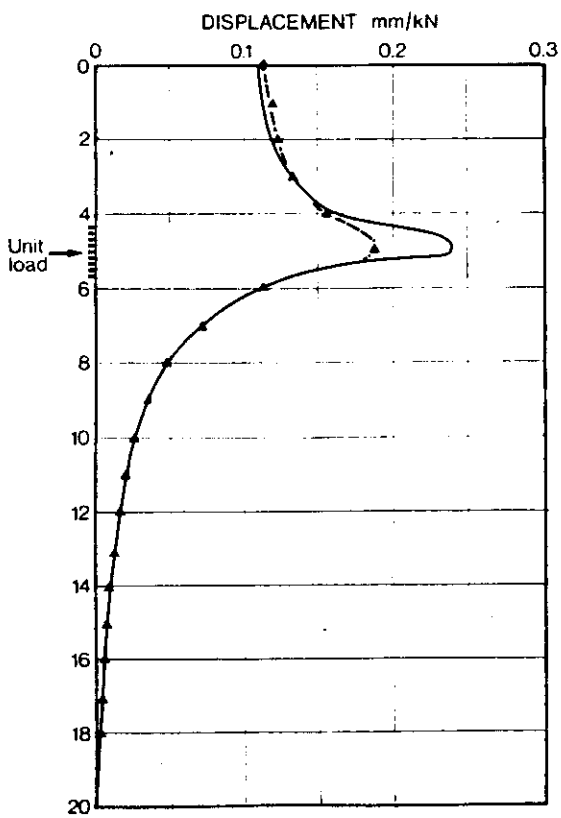

c) Displacement due to unit load at 5m depth

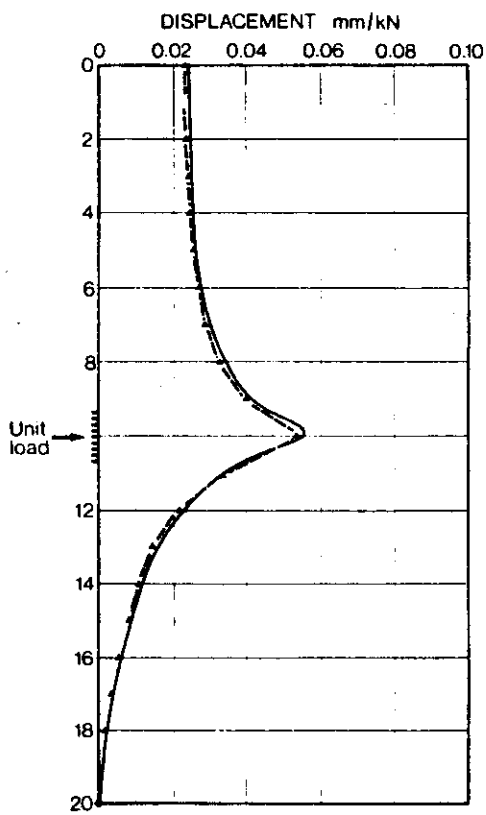

d) Displacement due to unit load at 10m depth

Figure 4 Approximation to accomodate non-linear variation in soil stiffness

will affect the flexibility matrix, and hence the stiffness matrix. This is particularly so for situations where a narrow excavation such as a trench will result in L/H ratios less than 1 where the soil behaviour is better modelled as a subgrade reaction. Therefore, in order to cater for situations between the extremes of L/H ratio, the stiffness matrix has been further modified by adding a single spring at each node with a spring stiffness calculated as EA/L where E is the soil stiffness and A is related to node spacing. For high L/H ratios the spring stiffness is small due to the large spring length and the stiffness matrix is virtually unchanged. For small L/H ratios the single spring stiffness becomes dominant and controls the calculated wall movements. Test comparisons were carried out with finite element computations (for an elastic soil which had a linearly increasing stiffness with depth) to determine the error due to this simplified assumption. The agreement was within 10% for L/H ratios in the range 0.3 to 0.6 and for L/H ratios greater than about 3. The largest differences occur for L/H ratios of about 1 when the maximum difference between the two methods is about 30%.

2.5 Soil strength limitations

The soil strength limitations are modelled using active and passive pressure states which may be represented at any depth z by

$$p_a \leqslant p \leqslant p_p \tag{6}$$

where p is the earth pressure, and p_a and p_p are the active and passive earth pressures defined by the following expressions

$$p_a = K_a p'_v - 2\sqrt{K_a}\, c + u \tag{7}$$

$$p_p = K_p p'_v - 2\sqrt{K_p}\, c + u \tag{8}$$

where K_a and K_p are the earth pressure coefficients, p'_v is the vertical effective stress, u is the pore water pressure and c the cohesion at depth z.

In the absence of wall friction and adhesion, Inequality (6) corresponds to a Rankine analysis. It can be shown that this represents a sufficient condition for stability of the soil, but not a

necessary condition. In many circumstances, it may be possible for the earth pressure at some points on the wall to lie outside these limits without the formation of a mechanism that can lead to failure of the wall.

The formation of a mechanism can be studied by analysis of a wedge of soil, as shown in Figure 5a. Coulomb showed that, in the absence of wall friction, the force between ground surface and depth z was limited thus

$$\int_0^z p_a \, dz \leqslant \int_0^z p \, dz \leqslant \int_0^z p_p \, dz \qquad (9)$$

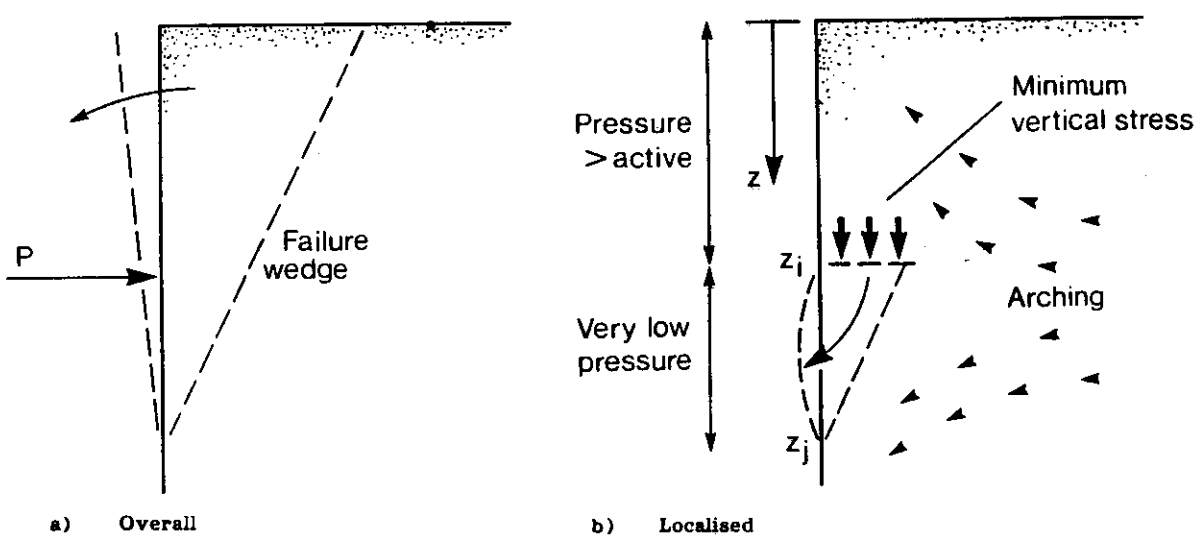

Figure 5 Mechanisms for active failure

The notation here is as in Inequality (6). Inequality (9) provides necessary conditions for the prevention of a mechanism which extends from depth z up to the ground surface. It is not, however, sufficient to prevent other localised mechanisms developing within the soil body.

In order to provide a good approximation to conditions which are both necessary and sufficient to prevent instability, the mechanism represented by Figure 5b has been studied. It is considered that this type of mechanism will not occur provided that at any depth $z_j > z_i$

$$\int_{z_i}^{z_j} p_{az}\, dz \leqslant \int_{z_i}^{z_j} p\, dz \leqslant \int_{z_i}^{z_j} p_{pz}\, dz \qquad (10)$$

where p_{az} at depth z between z_i and z_j is given by the expression

$$p_{az} = K_a \left[\sigma'_{vi\ min} + \int_{z_i}^{z} \gamma dz - u + u_i \right] - 2\sqrt{K_a}\ c + u \qquad (11)$$

In this expression u_i is the pore pressure and $\sigma'_{vi\ min}$ is the minimum vertical effective stress which could occur at depth z_i.

Similarly p_{pz} at depth z is given by

$$p_{pz} = K_p \left[\sigma'_{vi\ max} + \int_{z}^{z_i} \gamma dz - u + u_i \right] + 2\sqrt{K_p}\ c + u \qquad (12)$$

In this expression $\sigma'_{vi\ max}$ is the maximum vertical effective stress which could occur at depth z_i.

The minimum and maximum vertical effective stresses are not necessarily equal to the vertical effective stress induced by the overburden and surcharges. If arching occurs the vertical stress on the soil adjacent to the wall may vary greatly. If wall friction is ignored, however, the minimum and maximum vertical stresses at depth z_i are taken as being equal to

$$\sigma'_{vi\ min} = p'_i\ K_{ai} - 2\sqrt{K_{ai}}\ c_i \leqslant 0 \qquad (13)$$

$$\sigma'_{vi\ max} = p'_i\ K_{pi} + 2\sqrt{K_{pi}}\ c_i \qquad (14)$$

where p'_i is the horizontal effective stress acting at depth z_i and K_{ai}, K_{pi} and c_i are the earth pressure coefficients and the cohesion at depth

z_i. These equations provide an approximate method of representing local failure of the soil. Use of conditions (10) to (14) provides a conservative limitation on the amount of arching which can occur in the model.

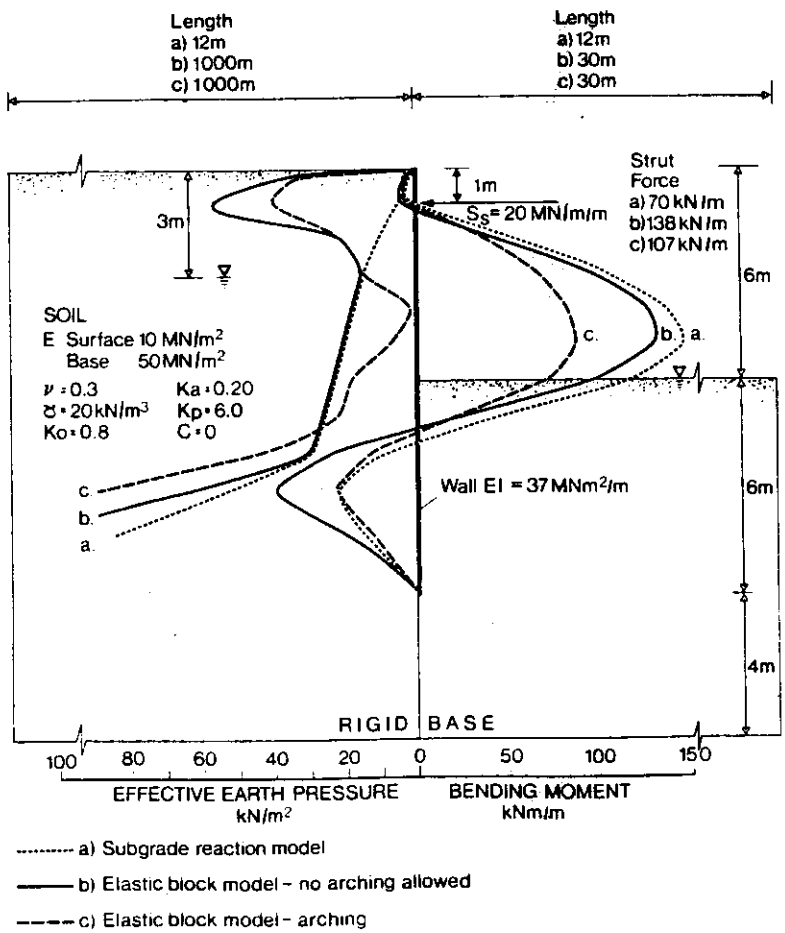

Figure 6 Effects of soil arching

During use of the computer program the designer may choose whether to use Inequality (6) or Inequality (10). It is believed that the latter is more reasonable and better reflects the actual situation as it permits a limited degree of arching to occur within the soil body. The effect of allowing arching on soil pressures and wall bending moments is illustrated in Figure 6. Results using Inequality (10) are referred to as arching. As the earth pressures near the strut are well above active pressure ($p > p_a$) the analysis has allowed the pressures at greater depth to reduce below the Rankine active pressure. This has markedly reduced the bending moments in the wall and the strut force.

Also shown in Figure 6 are results of computations carried out using a subgrade reaction model for soil stiffness. Soil spring stiffnesses were adjusted to give a similar wall displacement profile to that obtained from the elastic block method. As can be seen this simpler model has failed to predict an increase in earth pressures in the soil behind the strut. This has therefore led to an underestimate of the strut force and a slight overestimate of wall bending moments.

Application of the soil strength earth pressure limitations defined above is carried out by the program by computing nodal correction forces to restore acceptable pressure levels. To obtain convergence it has been found necessary to calculate displacement corrections from which the force corrections are obtained using the soil flexibility matrix. The displacement corrections are computed for each node and are associated with the plastic strain developed in the body of soil.

When displacement corrections are used the earth pressure at any node can still be influenced through the soil by the movement of the nodes below. However the earth pressure may be independent of the movement of the node itself and nodes above. This is illustrated by considering a failure surface as shown in Figure 7. The displacement correction applied to ensure that the limits are not violated at node q will cause a change of pressure but no displacement at node r, whilst at node p there will be a change of displacement but no change of

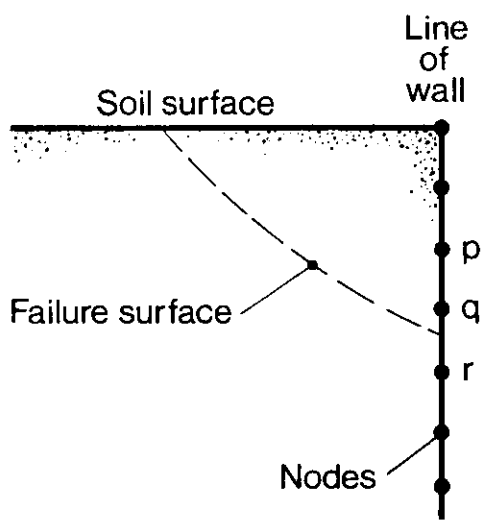

Figure 7 Failure surface in soil

pressure. This means that movement is taking place at constant stress on the failure surface whilst elastic conditions are still maintained separately in the blocks of material on either side of the failure surface.

To satisfy these conditions the displacement corrections are calculated using the following procedure which works downwards through each node starting at the soil surface.

(a) at the node (labelled here as i for convenience) calculate the approximate displacement correction that would cause the pressure at the node to change by the required amount to comply with the strength criteria.

(b) For each node j above node i calculate the displacement correction that is required to prevent a change of pressure at node j when the displacement at node i is corrected by the approximate displacement correction.

(c) Having completed (a) and (b) for all the nodes sum the displacement corrections to determine the total displacement correction for each node.

2.6 Excavation or Filling

The effect of excavation or filling is modelled by specifying the ratio of change in horizontal effective stress over change in vertical effective stress. This ratio is denoted by K_o and K_r which are used by the analysis as follows:

(a) K_o for determining the horizontal effective stress in either the initialisation stage or in filled material.

(b) K_r for determining the change in horizontal effective stress due to a change in the vertical effective stress which arises as a result of either excavation or filling. Generally, K_r should be set to

$\nu/(1-\nu)$ but in the situation where σ'_v is being increased to above the preconsolidation pressure a value of K_r of about 1-Sin ϕ' may be more appropriate where ϕ' is the angle of internal shearing resistance.

2.7 Struts or Anchors

Struts or anchors can be installed at any node at any stage during the analysis. As shown in Figure 2 the struts are specified as having a prestress force P_s and a stiffness S_s in terms of force/unit displacement. To model the effect of a moment being applied to the wall by a strut or an anchor a lever arm L_s and inclination α_s can also be specified as shown in the figure. This feature is mainly used to model the effect of an inclined strut or anchor applying the force eccentrically to the wall section.

Based on the geometry defined in Figure 2 the force P and moment M applied at the node by the strut is given by

$$P = P_s \text{Cos}\,\alpha_s + \delta S_s \text{Cos}^2\,\alpha_s + \theta S_s L_s \text{Cos}\,\alpha_s \text{Sin}\,\alpha_s \quad (15)$$

$$M = P_s L_s \text{Sin}\,\alpha_s + \delta S_s L_s \text{Cos}\,\alpha_s \text{Sin}\,\alpha_s + \theta S_s L_s^2 \text{Sin}^2\,\alpha_s \quad (16)$$

In these expressions δ is the horizontal deflection of the node and θ the rotation of the node since the introduction of the strut.

These equations can be written in the form of matrices that represent all struts currently acting on the wall as

$$[P] = [P_s \text{Cos}\,\alpha_s] + [S_{sh}][\delta] + [S_{sc}][\theta] \quad (17)$$

$$[M] = [P_s L_s \text{Sin}\,\alpha_s] + [S_{sc}][\delta] + [S_{sm}][\theta] \quad (18)$$

where the strut stiffness matrices are diagonal and equal to

$$[S_{sh}] = [S_s \text{Cos}^2 \alpha_s] \tag{19}$$

$$[S_{sc}] = [S_s L_s \text{Cos}\, \alpha_s \text{Sin}\, \alpha_s] \tag{20}$$

$$[S_{sm}] = [S_s L_s^2 \text{Sin}^2 \alpha_s] \tag{21}$$

The effect of the struts are incorporated into the analysis by matrix addition of the expressions given above to those given in equations (1) and (2). Elimination of $[\theta]$ gives the following expression which is comparable to equation (3)

$$[P] = [D] + [S][\delta] \tag{22}$$

where the new stiffness matrix for the wall [S] including the effect of the struts, and the effect of the prestress [D] are given by

$$[S] = [C] + [S_{sh}] - \left[[A] + [S_{sc}] \right]^T \left[[B] + [S_{sm}] \right]^{-1} \left[[A] + [S_{sc}] \right] \tag{23}$$

$$[D] = [P_s \text{Cos}\, \alpha_s] + \left[[A] + [S_{sc}] \right]^T \left[[B] + [S_{sm}] \right]^{-1} \left[[P_s L_s \text{Sin}\, \alpha_s] \right] \tag{24}$$

Of particular interest is the special case of a strut inclined at 90° to the wall for which equation (16) reduces to

$$M = P_s L_s + \theta S_s L_s^2 \tag{25}$$

which allows moment fixity to be modelled at any node.

2.8 Surcharges

The modelling of surcharges is often required to include the effect of nearby foundations or loadings. In the analysis two types of

surcharge can be specified to act on either side of the wall at any stage during construction, either a uniformly distributed load (UDL) or a strip load of finite width B acting at a distance A from the wall with a pressure q (see Figure 8). Both types of surcharge can be applied at or below the ground surface but the analysis assumes that a surcharge has no effect above its level of application.

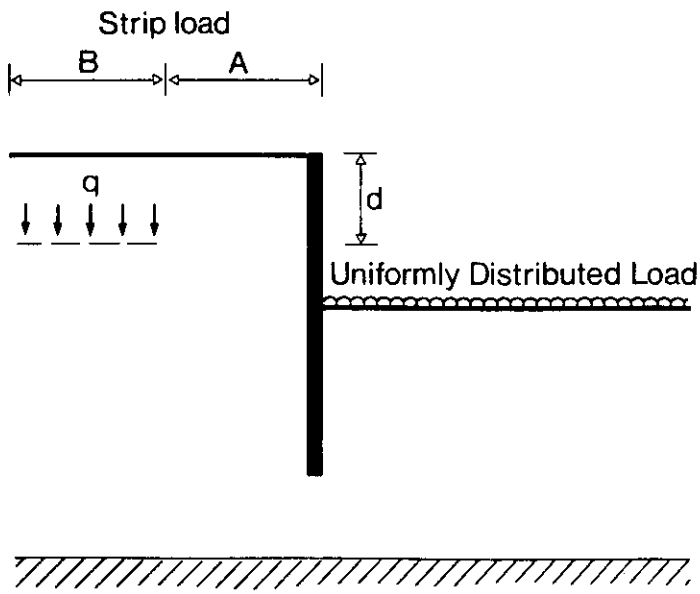

Figure 8 Surcharge geometry

The effects of either type of surcharge on the behaviour of the wall are calculated by the computer program in two steps.

a) Computing the changes in earth pressures acting on the wall before any further displacement occurs.

b) computing the changes to the active and passive earth pressure limitations.

For the case of a UDL the change in earth pressure on the wall due to the surcharge load is simply evaluated as qK_r. For a strip load however the change in stress is difficult to determine because the horizontal stress is extremely sensitive to the variation, with depth, of the soil stiffness. Two extremes have therefore been considered.

For the case where the Young's modulus for the soil is constant for a depth several times greater than the width of the surcharge the Boussinesq equations may be used to derive horizontal stresses in the ground. The pressures therefore on a rigid (ideally frictionless) vertical boundary would be double the Boussinesq values.

For the case where the stiffness increases sharply at a depth less than the width of the surcharge the load will appear to the more flexible soil to act rather like a UDL. For the stiffer soil the effect of the surcharge load will still appear as the Boussinesq pressure.

For both cases the analysis calculates the change of pressure on the wall before further movement using the equation

$$p = 2K_s \Delta\sigma_{hB} \qquad (26)$$

where $\Delta\sigma_{hB}$ is the change of horizontal stress according to the Boussinesq equations and K_s is a correction factor specified by the user.

For the first case K_s should be taken as 1.0. For other cases K_s can have a large range of values, the evaluation of which is beyond the scope of the analysis. However if the strip load is wide compared with its distance from the wall and the depth of the deforming soil, a value of $K_s = \nu/(1-\nu)$ will give results equivalent to loading with a UDL with $K_r = \nu/(1-\nu)$.

Initial surcharges, which are present before construction of the wall, are modelled in the same way as other surcharges. However, in selecting K_s the effects of construction of the wall on existing horizontal stresses must also be considered.

The effects of the surcharge loading on the active and passive pressure limits is also highly dependent on the type of surcharge being considered. For a UDL they are simply calculated as qK_a and qK_p respectively. However for a strip load the effect is more difficult to determine and depends on many factors.

Considerable efforts have been made to formulate a relatively simple approximation to model the effect of a strip load on the active pressure limits. Parametric studies have been carried out using straight line and log spiral shaped failure surfaces for soil that has constant properties with depth. The ranges of variables considered were as follows; ϕ' from 15° to 60°, $q/\gamma B$ from 0.33 to 5 and A/B from 0 to 2. The results showed that the straight line and log spiral methods usually gave very similar results. It is considered important that whatever approximation is chosen should be generally conservative, and in the case of active pressure this should be achieved by maximising the pressure near the top of the soil.

From purely theoretical considerations the approximation illustrated in Figure 9a was developed to represent the change in the active pressure limit. This shows the shape of the pressure limit diagram and the criteria for calculation. It should be noted that if the width of the load (B) is small the diagram will become triangular. This distribution of

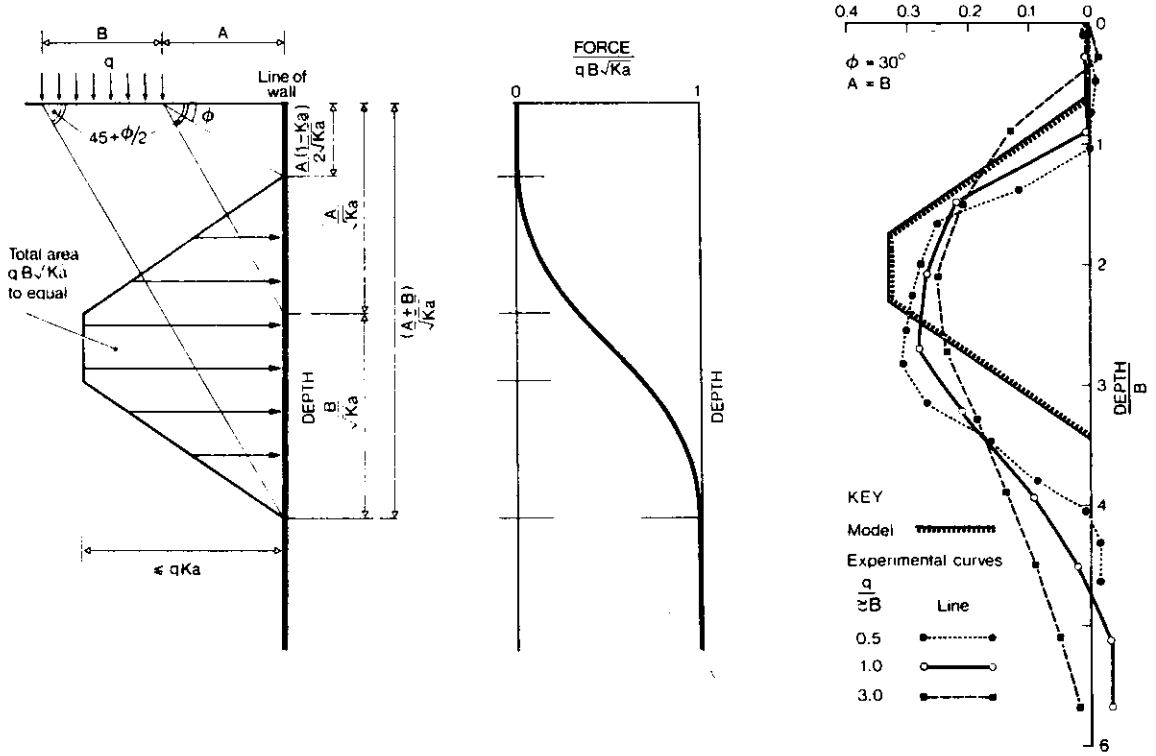

a) Approximation to represent the change in active pressure limitation due to surcharge

b) Distribution of change in active force

c) Comparison of approximation with results of parametric study

Figure 9 Effect of surcharge loading on the active pressure limit

pressure is then used to modify the active pressure limit. Comparison between the theoretical pressure limit change distribution and several curves taken from the parametric study is presented in Figure 9c. It is seen that the theoretical solution agrees well with the correct solutions and is generally conservative.

If K_a varies with depth it is considered conservative to choose a mean value of K_a between any depth z and the level of the surcharge and then impose the criteria that the active force due to the surcharge, down to depth z be equal to the force derived from the diagram in Figure 9b. This is then subjected to the further limitation that the pressure never exceeds qK_{az} at any depth, where K_{az} is the active earth pressure coefficient at depth z.

The effects of a strip load on the passive pressure are not as easily represented by a simple pressure diagram. It is generally conservative to locate the increase in passive resistance at a point as low as possible. However, in some instances, for example where a floor slab is preventing toe failure of a wall, this is unrealistic and the effect on the passive pressure limits due to a strip load must be specified directly.

3 THE PROGRAM - INPUT AND OUTPUT

The method of analysis described in the previous section has been incorporated into a computer program that has been available for use by the Geotechnics group of Ove Arup and Partners for several years. The program in its present form is the result of continual development and improvement, particularly with regard to the input and output facilities and is now at a stage where it can be used by specialist engineers as part of the general design process.

Input to the program is completely interactive. The data are inserted in steps that represent stages of construction for which the program prompts for every variable. Where possible the data are checked to ensure that they are reasonable and possible.

Output from the program includes earth pressures, displacements, wall shear forces and bending moments. These can also be presented graphically. As an example, Figure 10 shows the results of the problem presented in Figure 6 for the elastic soil block method with no arching permitted.

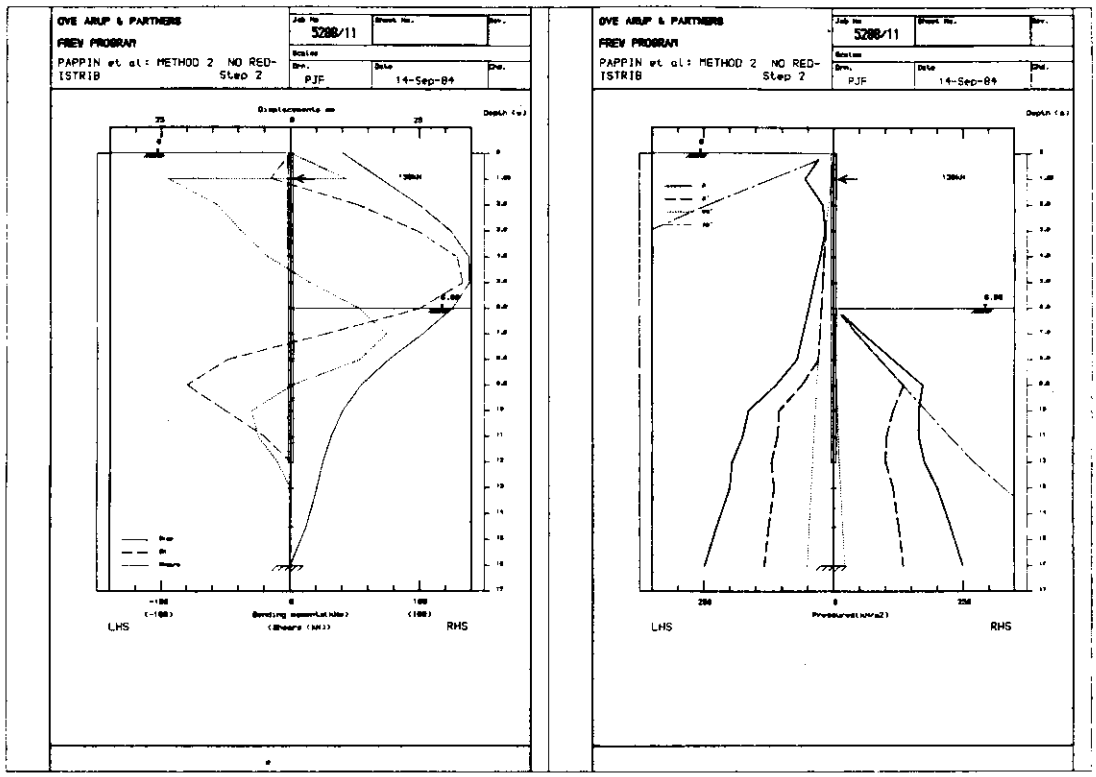

Figure 10 Example of computer program graphical output

4 EXAMPLES

In order to demonstrate how the method of analysis can be applied three examples are included below. The first is a classical problem which has been analysed as part of the general verification of the method. The second is a case where predictions were made during the design and subsequently displacements were measured during construction. Finally, the third case is an unusual problem included to illustrate the versatility of the analysis.

4.1 Rotation of a rigid wall

In 1934 Terzaghi reported the results of a now classical series of tests on the lateral pressures of dry sand against a retaining wall. A rigid wall was rotated about its base and the changes of earth pressure on the wall were recorded. The results of the tests together with some additional tests performed at Princeton are presented in NAVFAC DM7 (1971) which have been redrawn on Figure 11b. This problem was modelled by the analysis using the geometry and soil properties shown in Figure 11a. Results are presented in terms of the ratio K derived from the horizontal force (P_H). This force was calculated assuming that it acts at a third of the wall height above the base and gives a moment equal to the moment due to the calculated earth pressures.

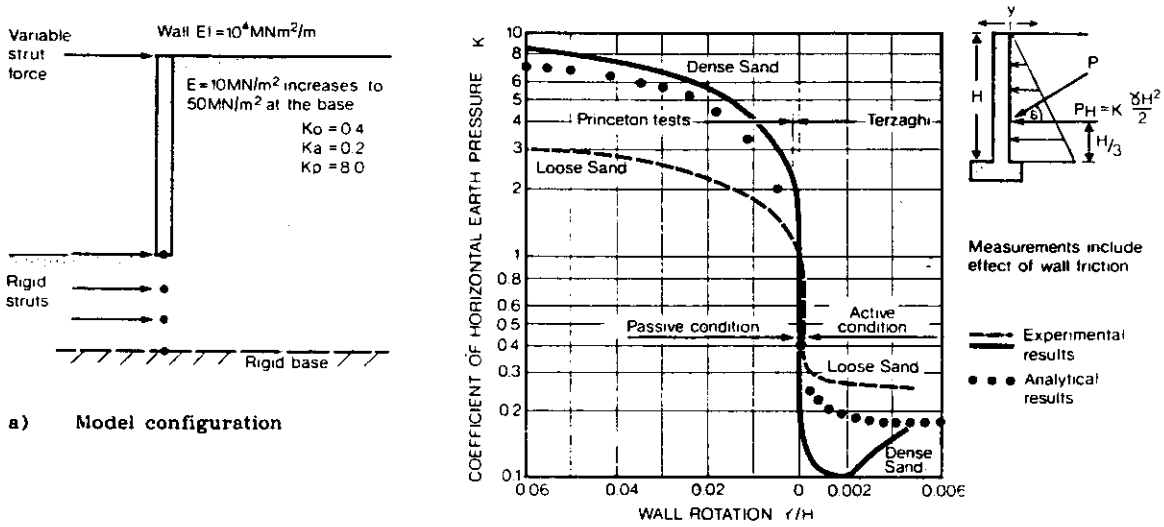

Figure 11 Rotation of a rigid wall

The results of the analysis give very similar results to those reported. In particular a smooth curve is computed for the variation of K with rotation, despite the use of a simple linear elastic/plastic model. This occurs because plastic yield is at first local to the top of the wall and gradually spreads downwards.

4.2 A multiple strutted excavation in soft clay

This problem is illustrated in Figure 12a. At the site about 2m of fill

overlies 26m of soft to firm clay over stiff to hard clay. Undrained shear strengths measured by a shear vane for the soft clay are also given. Predictions were made for the excavation using these results to represent the strength properties of the clay. To estimate the stiffness of the clay an E/c_u ratio of 750 was used during each stage of the construction but was reduced in the final stage to represent the large strain behaviour of the clay. The other parameters used in the analysis are also given in the figure.

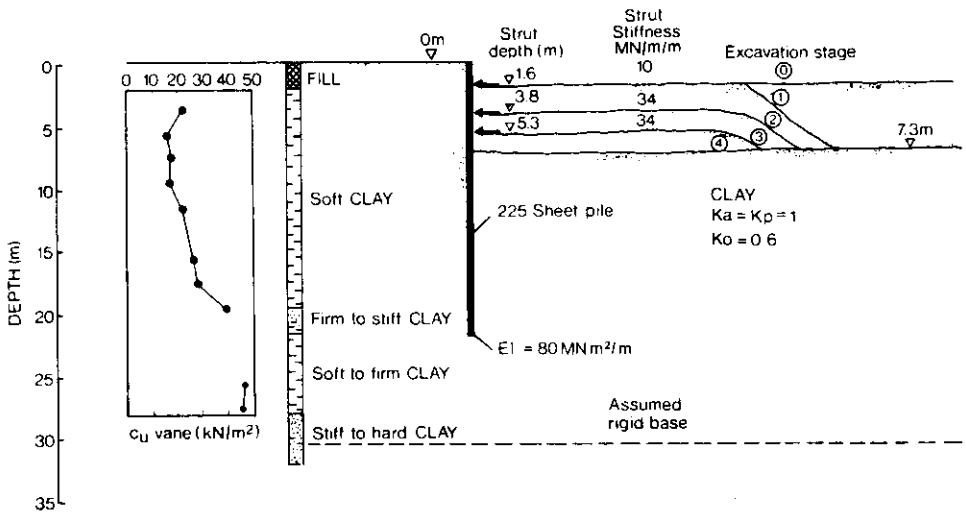

a) **Details of excavation**

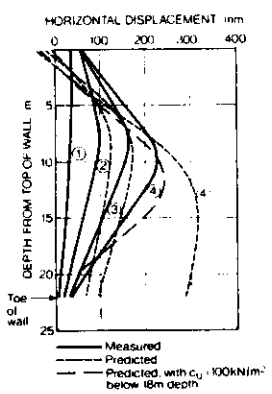

b) **Comparison between predictions and measurements**

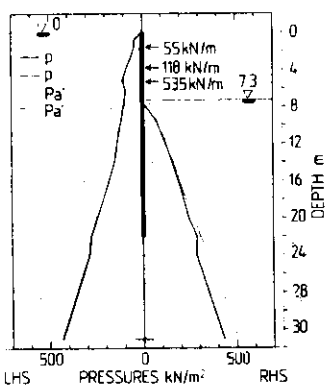

c) **Predicted earth pressures at stage 4**

Figure 12 A multiple strutted excavation in soft clay

The wall displacements predicted for each stage of construction are shown in Figure 12b and earth pressures for the final stage of analysis are shown in Figure 12c. The earth pressures show that arching was expected to occur below the excavation level on both sides of the wall, the pressure reducing below p_a to the left of the wall and increasing above p_p to the right.

Since the predictions were made the excavation has been completed to stage 4 during which, inclinometers installed along the line of the wall were used to measure displacements. Results have been published by Davies and Walsh (1983) and have been reproduced for each stage in Figure 12b. It can be seen that the predicted and measured displacements agree quite well for construction stages 2 and 3 but for the final stage they do not appear to agree well. This is attributed to the base of the wall moving much less than predicted because of the influence of the layer of firm to stiff clay below 18m depth. This was initially modelled as being soft clay since there was some doubt about its continuity and it was considered conservative to ignore it. Re-analysis of the problem was therefore carried out with the undrained shear strength of the clay increased to 100kN/m^2 below a depth of 18m. The final displacements for this case are also shown in Figure 12b and shows much better agreement with measurements. Underprediction of displacements near the top of the wall are considered to result from the use in the analysis of struts stiffer than those used in construction.

For the purposes of design this analysis is quite acceptable. The magnitudes of the displacements and wall bending moments are all well predicted. It is these parameters that influence the choice of wall type, excavation procedure and strutting arrangement.

4.3 Short wall restrained by a raft

Figure 13 illustrates an example of an analysis to investigate the behaviour of a short bored pile wall restrained by a 2m thick raft. Figure 13a shows the stages of construction which comprise a general excavation of 9.5m followed by the installation of a contiguous bored pile retaining wall. Subsequently a raft will be cast to one side of, and directly connected to, the top of the wall. A further excavation of 7m to the right hand side of the wall will allow the installation of a lower level raft. The behaviour of the wall during this excavation is the subject of the example.

The parameters used to represent the wall, the soil and the upper raft are given in Figures 13b and 13c. The high initial stresses assumed to

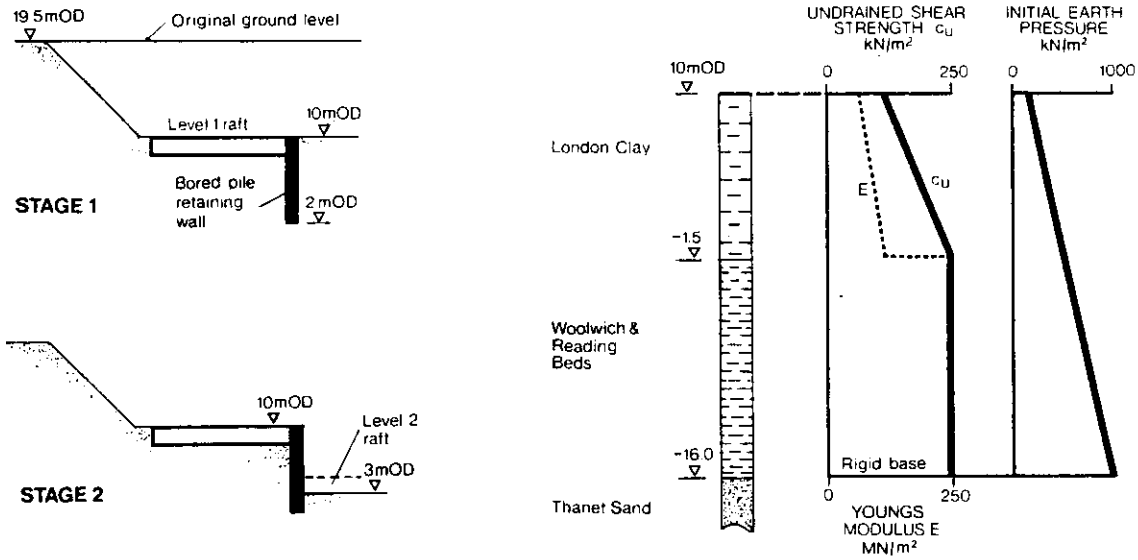

a) Construction sequence

b) Soil properties used for the analysis

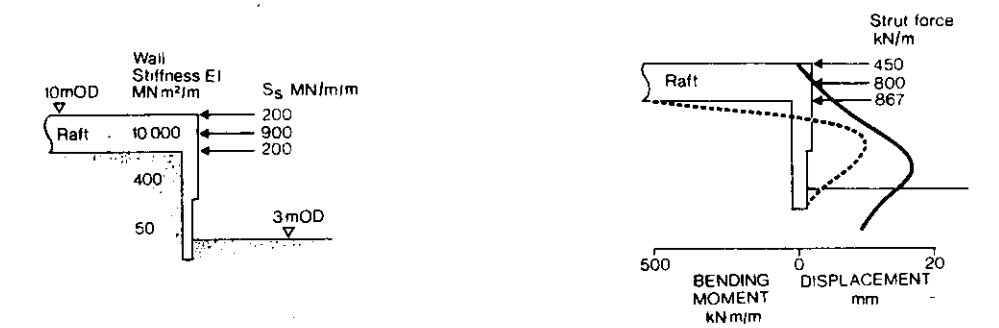

c) Raft and wall properties used for the analysis

d) Results of the analysis

Figure 13 Short bored pile wall restrained by a raft

be acting on the wall were obtained by considering the probable soil stress paths during the first part of the 9.5m excavation. Drained excavation was assumed for the initial excavation but all subsequent excavation was assumed to be undrained. The bending resistance and horizontal restraint of the raft was represented by 3 struts acting on the top three nodes. The wall stiffness (EI) was also increased for the depth of the raft. Results of the analysis are given in Figure 13d from which it can be seen that rotation of the wall is predicted with a maximum deflection of 18mm near the base and a maximum bending moment of about 600kNm/m.

During construction it is planned to monitor movements of the wall for comparison with predictions.

5 VALIDATION

In the previous sections an analysis method has been presented and examples given of its use. However, to be of use it is necessary to determine the reliability of the analysis in predicting the required design parameters.

Validation by comparison with actual results is a difficult process. The parameters used in the analysis control the predicted behaviour and for a back analysis of a problem with a known result it is usually possible to match the measured response by manipulating the parameters. However, this does not directly test the analysis itself, but does allow an assessment to be made of the sensitivity of the analysis to the parameters.

An improvement on a back analysis is a design prediction which is subsequently verified by measurement. The multiple strutted excavation presented above is an example of this. However, it can be seen that the design prediction for the actual problem was rather poor but the consequences of this error in prediction were not significant. This was because the designer was not trying to achieve an exact prediction but rather to explore what may happen. The differences between predictions and measurements in this instance are, therefore, quite acceptable.

Several attempts have also been made to test the program against classical or more rigorous solutions. An example has been given above for a rigid wall rotating about its base where the analysis was able to accurately model the measured behaviour. Other comparisons have also been made between predictions from this analysis and those using finite element computations. No examples are given here but generally reasonable agreement has been found between the two methods.

6 EFFECTS BEYOND THE SCOPE OF THE ANALYSIS

The analysis cannot directly model the effects of parameters that change with time such as the change from undrained to drained behaviour, or the effects of creep. This is important, for example, in the case of a retaining wall in stiff clay where in the short term the soil will behave

in an undrained manner but in the long term drained behaviour of the soil is relevant. Wall and permanent strutting systems are usually installed quickly and strut loads tend to increase as the soil approaches the long term condition. The increases in strut load will therefore be a function of the change in pressure acting on the wall resulting from dissipation of pore pressures developed within the soil due to excavation. The analysis cannot calculate these changes and therefore the designer must specify them directly to enable the analysis to model their effect.

True non linear behaviour is not directly modelled by the analysis even though a linear elastic/plastic model is used. In reality soil behaviour is always non linear and where this effect is significant, alternative methods should be used.

The wall itself may also behave in a non linear manner. If required, however, a simple linear elastic/plastic model could be included in the analysis presented here.

7 SUMMARY

a) A numerical method of analysis for flexible retaining walls that is sufficiently simple and cheap to be used in the general design process has been presented.

b) The unusual but very powerful features of the analysis are the ways in which soil stiffness and earth pressure limits are modelled.

c) The soil stiffness is generated from considering a block of elastic material rather than the commonly used series of independent springs.

d) The earth pressure limits are determined from consideration of forces resisted by or applied to the soil rather than simple comparisons with active and passive pressure limits.

e) The importance of good input and output facilities has been emphasised.

f) Examples have been given to demonstrate the use and range of the analysis.

g) Thorough validation of the analysis is difficult.

8 ACKNOWLEDGEMENTS

The paper presented here is an abridged version of a paper that was presented at NUMETA 85, Swansea in January 1985.

The authors wish to acknowledge the efforts of their many colleagues who have contributed to the development and testing of the computer program based on the analysis presented here.

REFERENCES

VAZIRI, H., SIMPSON, B., PAPPIN, J.W., & SIMPSON, L. (1982). Integrated forms of Mindlin's equations. Vol. 32, No. 3 Geotechnique. ICE London.

PAPPIN, J.W., SIMPSON, B., FELTON, P.J. & RAISON, C. (1985). Numerical analysis of flexible retaining walls. Proc. Conf. Num. Methods in Eng. Theory and Applications, Swansea.

DAVIES, R.V. & WALSH, N.M. (1983). Excavations in Singapore marine clay. Int. Seminar on Construction Problems in Soft Soils. Nanyang Technological Inst., Singapore.

NAVFAC - DM7 1971, Design Manual. US Naval Pubs. and Forms Cntr., Philadelphia Pa. 19120 U.S.A.